Cellular/Molecular

Sustained G_q-Protein Signaling Disrupts Striatal Circuits via JNK

Luigi Bellocchio,[1] Andrea Ruiz-Calvo,[1] Anna Chiarlone,[1] Magali Cabanas,[2] Eva Resel,[1] Jean-René Cazalets,[2] Cristina Blázquez,[1] Yoon H. Cho,[2] Ismael Galve-Roperh,[1] and Manuel Guzmán[1]

[1]Department of Biochemistry and Molecular Biology I, Centro de Investigación Biomédica en Red sobre Enfermedades Neurodegenerativas (CIBERNED), Instituto Ramón y Cajal de Investigación Sanitaria (IRYCIS), and Instituto Universitario de Investigación Neuroquímica (IUIN), Complutense University, 28040 Madrid, Spain, and [2]Institute of Cognitive and Integrative Neuroscience of Aquitaine, University of Bordeaux, 33615 Pessac Cedex, France

The dorsal striatum is a major input structure of the basal ganglia and plays a key role in the control of vital processes such as motor behavior, cognition, and motivation. The functionality of striatal neurons is tightly controlled by various metabotropic receptors. Whereas the G_s/G_i-protein-dependent tuning of striatal neurons is fairly well known, the precise impact and underlying mechanism of G_q-protein-dependent signals remain poorly understood. Here, using different experimental approaches, especially designer receptor exclusively activated by designer drug (DREADD) chemogenetic technology, we found that sustained activation of G_q-protein signaling impairs the functionality of striatal neurons and we unveil the precise molecular mechanism underlying this process: a phospholipase C/Ca^{2+}/proline-rich tyrosine kinase 2/cJun *N*-terminal kinase pathway. Moreover, engagement of this intracellular signaling route was functionally active in the mouse dorsal striatum *in vivo*, as proven by the disruption of neuronal integrity and behavioral tasks. To analyze this effect anatomically, we manipulated G_q-protein-dependent signaling selectively in neurons belonging to the direct or indirect striatal pathway. Acute G_q-protein activation in direct-pathway or indirect-pathway neurons produced an enhancement or a decrease, respectively, of activity-dependent parameters. In contrast, sustained G_q-protein activation impaired the functionality of direct-pathway and indirect-pathway neurons and disrupted the behavioral performance and electroencephalography-related activity tasks controlled by either anatomical framework. Collectively, these findings define the molecular mechanism and functional relevance of G_q-protein-driven signals in striatal circuits under normal and overactivated states.

Key words: cJun N-terminal kinase; G-protein-coupled receptor; medium spiny neuron; striatal circuit

Significance Statement

The dorsal striatum is a major input structure of the basal ganglia and plays a key role in the control of vital processes such as motor behavior, cognition, and motivation. Whereas the G_s/G_i-protein-dependent tuning of striatal neurons is fairly well known, the precise impact and underlying mechanism of G_q-protein-dependent signals remain unclear. Here, we show that striatal circuits can be "turned on" by acute G_q-protein signaling or "turned off" by sustained G_q-protein signaling. Specifically, sustained G_q-protein signaling inactivates striatal neurons by an intracellular pathway that relies on cJun *N*-terminal kinase. Overall, this study sheds new light onto the molecular mechanism and functional relevance of G_q-protein-driven signals in striatal circuits under normal and overactivated states.

Introduction

The basal ganglia are a series of interconnected subcortical nuclei including the striatum (caudate and putamen in primates), the globus pallidus (internal and external segments), the subthalamic nucleus, and the substantia nigra (pars reticulata and pars compacta). They are a key node for many behavioral and neurobio-

Received April 8, 2016; revised Aug. 1, 2016; accepted Aug. 25, 2016.

Author contributions: L.B., A.R.-C., M.C., J.-R.C., Y.H.C., I.G.-R., and M.G. designed research; L.B., A.R.-C., A.C., M.C., E.R., and C.B. performed research; L.B., A.R.-C., A.C., M.C., E.R., J.-R.C., C.B., Y.H.C., I.G.-R., and M.G. analyzed data; L.B., A.R.-C., Y.H.C., I.G.-R., and M.G. wrote the paper.

This work was supported by the Spanish Ministerio de Economía y Competitividad (MINECO/FEDER; Grants SAF2012-35759 and SAF2015-64945-R to M.G.) and Comunidad de Madrid (Grant S2010/BMD-2308 to M.G.). L.B. was supported by an EMBO Long-Term Fellowship (ALTF 975-2011). A.R.-C. and A.C. were supported by the Spanish Ministerio de Economía y Competitividad (FPI Program). M.C. was supported by the French Ministry of Higher Education and Research. We thank Elena García-Taboada and Mar Martín-Fontecha for expert technical assistance and Giovanni Marsicano, Joseph F. Cheer, Daniela Cota, and Jean M. Revest for critical reading of the manuscript.

The authors declare no competing financial interests.

Correspondence should be addressed to either Manuel Guzmán or Luigi Bellocchio, Department of Biochemistry and Molecular Biology I, School of Biology, Complutense University, Calle José Antonio Novais 12, 28040 Madrid, Spain. E-mail: mguzman@quim.ucm.es or luigi.bellocchio@inserm.fr.

DOI:10.1523/JNEUROSCI.1192-16.2016

 0270-6474/16/3610611-14$15.00/0

Table 1. Cell signaling inhibitors used in combination with CNO for cell viability and Western blot analyses

Product	Target	Final concentration	Vehicle	Supplier
U73122	PLC	5 μM	DMEM 0.5% DMSO	Santa Cruz Biotechnology
U73343	PLC (inactive)	5 μM	DMEM 0.5% DMSO	Santa Cruz Biotechnology
BAPTA-AM	Intracellular Ca^{2+}	2 μM	DMEM 0.5% DMSO	Santa Cruz Biotechnology
2-APB	IP_3 receptor	100 μM	DMEM 0.5% DMSO	Santa Cruz Biotechnology
*Bis*indolylmaleimide	PKC	2 μM	DMEM 0.5% DMSO	Sigma-Aldrich
SP600125	JNK	12.5 μM	DMEM 0.5% DMSO	Santa Cruz Biotechnology
U0126	MEK	25 μM	DMEM 0.5% DMSO	Merck Millipore
LY294002	PI3K	10 μM	DMEM 0.5% DMSO	Cell Signaling Technology
Akti-1/2	Akt	100 nM	DMEM 0.5% DMSO	Calbiochem
Rapamycin	mTORC1	500 nM	DMEM 0.5% DMSO	Tecoland
ZVAD-FMK	Pan caspases	5 μM	DMEM 0.5% DMSO	Santa Cruz Biotechnology
Pepstatin A/E64D	Ca^{2+} proteases	15/20 μM	DMEM	Sigma-Aldrich
PF431396	FAK/PYK2	5 μM	DMEM 0.5% DMSO	Tocris Bioscience

logical processes such as motor activity, cognitive functions, and affective control. The vast majority (~95%) of neurons within the striatum are GABAergic medium spiny neurons (MSNs), which receive glutamatergic inputs primarily from the cortex and from specific thalamic nuclei (Kreitzer, 2009). MSNs differ in their neurochemical composition and form two major efferent pathways. The direct pathway consists of MSNs expressing the dopamine D_1 receptor (D_1R), substance P, and dynorphin. It mainly projects to the substantia nigra pars reticulata and the internal segment of the globus pallidus. The indirect pathway is composed of MSNs expressing the dopamine D_2 receptor (D_2R), adenosine A_{2A} receptor, and enkephalin. It mainly projects to the external segment of the globus pallidus, which, in turn, projects to the subthalamic nucleus. Many conceptual models hypothesize that these two MSN populations oppose one another both mechanistically and functionally (Nelson and Kreitzer, 2014). However, obtaining empirical evidence to support their roles has proven difficult because these cell populations are physically intermingled and morphologically indistinguishable. The implementation of optogenetics to control neuronal activity with exquisite temporal resolution using engineered opsins has provided an expanding platform for decoding striatal functions (Kreitzer and Berke, 2011; Freeze et al., 2013). More recently, the designer receptor exclusively activated by designer drug (DREADD) technology has been developed as a powerful tool for controlling neuronal activity remotely (Jennings and Stuber, 2014; Lee et al., 2014). This chemogenetic method is based on the expression of engineered G-protein-coupled receptors (GPCRs) that are selectively and potently activated by systemically bioavailable, brain-penetrant and otherwise pharmacologically inert ligands such as clozapine-*N*-oxide (CNO) (Armbruster et al., 2007; Alexander et al., 2009). DREADDs have no detectable constitutive activity and, by using conserved and canonical GPCR-dependent signaling pathways, allow a spatiotemporally selective and physiological manipulation of metabotropic signaling pathways.

Metabotropic signaling is absolutely necessary for the proper functioning of the striatum. Neurotransmitters/neuromodulators such as dopamine, glutamate, adenosine, acetylcholine, and endocannabinoids control the activity and plasticity of MSNs by engaging various GPCR families. Specifically, the main dopamine receptors present in MSNs, namely D_1R and D_2R, are coupled to G_{olf} and G_i proteins, respectively, and the detailed roles of these signaling axes on striatal functions have been reported (Ferguson et al., 2011; Bock et al., 2013; Farrell et al., 2013; Ferguson et al., 2013). G_q-coupled receptors such as metabotropic glutamate $mGlu_{1/5}$ receptors and muscarinic acetylcholine $M_{1/3/5}$ receptors are also very important in the control of MSN excitability and an overactive G_q-protein-driven signaling has been shown to occur in various models of basal ganglia-related diseases such as Huntington's disease and drug addiction (Conn et al., 2005; Kreitzer, 2009; Ribeiro et al., 2011; Girault, 2012; Cahill et al., 2014). However, the precise impact and mode of action of G_q-protein signaling on MSNs have not been clarified so far. Therefore, here, we used different approaches, especially the DREADD chemogenetic technology, to examine the molecular mechanisms and physiopathological relevance of G_q-protein signaling in direct-pathway and indirect-pathway MSNs. Our findings unveil an unprecedented molecular mechanism of G_q-protein-evoked neuronal inactivation that is relevant in the disruption of striatal functions *in vivo*.

Materials and Methods

Animals

We used mutant mice and their corresponding wild-type littermates in which Cre recombinase expression was driven by the D_1R promoter (Monory et al., 2007; colony founders provided by Günther Schütz, German Cancer Research Center), the D_2R promoter (colony founders provided by University of California Davis Knockout Mouse Project Repository, Davis, CA), or both the D_1R and D_2R promoters (generated by crossing the aforementioned D_1R-Cre and D_2R-Cre mouse lines). All lines were in the C57BL/6N background. Wild-type C57BL/6N mice were purchased from Harlan Laboratories. Animal housing, handling, and assignment to the different experimental groups were conducted as described previously (Blázquez et al., 2011). All experimental procedures used were performed in accordance with the guidelines and with the approval of the Animal Welfare Committee of Madrid Complutense University according to the European Commission directives.

Viral vectors

G_q-coupled human M_3 muscarinic DREADD (hM3Dq) fused to mCherry (provided by Brian L. Roth, University of North Carolina, Chapel Hill, NC; Alexander et al., 2009) or mCherry alone was subcloned in a recombinant adeno-associated virus (rAAV) expression vector with a minimal CAG promoter (for generalized expression) or in a CAG-DIO vector (for Cre-dependent expression) using standard molecular biology techniques. For cell-specific ablation, a mCherry-FLEX-DTA cassette (Addgene plasmid #58536, provided by Naoshige Uchida, Harvard University) was cloned in a CAG-DIO-rAAV vector. All vectors used were of an AAV1/AAV2 mixed serotype and were generated by calcium phosphate transfection of HEK-293T cells and subsequent purification as described previously (Monory et al., 2006).

DREADD-induced neuronal manipulation in vivo

Eight-week-old male C57BL/6N mice were injected stereotaxically with CAG-hM3Dq-mCherry-rAAV or control CAG-rAAV (in 1.5 μl of PBS) aimed at targeting the dorsal striatum. Each animal received 1 bilateral

Table 2. Statistical test used for each set of data

Figure	Conditions	*n*	Analysis (*post hoc*)	Factor analyzed	*F*-value	*p*-value
2A	Vehicle vs CNO/WT vs mutants	6–10	Two-way ANOVA (Bonferroni)	Genotype	$F_{(1,55)} = 6.23$	<0.05
2A	Vehicle vs CNO/WT vs mutants	6–10	Two-way ANOVA (Bonferroni)	CNO treatment	$F_{(3,55)} = 10.28$	<0.01
2A	Vehicle vs CNO/WT vs mutants	6–10	Two-way ANOVA (Bonferroni)	Genotype × CNO treatment	$F_{(3,56)} = 8.15$	<0.01
2B	Vehicle vs CNO/WT vs mutants	6–10	Two-way ANOVA (Bonferroni)	Genotype	$F_{(3,57)} = 1.36$	>0.05
2B	Vehicle vs CNO/WT vs mutants	6–10	Two-way ANOVA (Bonferroni)	CNO treatment	$F_{(1,57)} = 8.37$	<0.01
2B	Vehicle vs CNO/WT vs mutants	6–10	Two-way ANOVA (Bonferroni)	Genotype × CNO treatment	$F_{(3,57)} = 1.81$	>0.05
2D	Acute vs chronic	4–5	One-way ANOVA (Tukey)	CNO treatment	$F_{(7)} = 11.05$	<0.01
2E	Wake acute vs chronic	8–10	One-way ANOVA (Tukey)	CNO treatment	$F_{(7)} = 2.20$	<0.05
2E	Slow wave sleep acute vs chronic	7–10	One-way ANOVA (Tukey)	CNO treatment	$F_{(7)} = 4.32$	<0.01
2E	REM sleep acute vs chronic	7–9	One-way ANOVA (Tukey)	CNO treatment	$F_{(7)} = 2.12$	0.05
3B	Vehicle vs CNO/WT vs mutants	6–10	Two-way ANOVA (Bonferroni)	Genotype	$F_{(3,56)} = 1.40$	>0.05
3B	Vehicle vs CNO/WT vs mutants	6–10	Two-way ANOVA (Bonferroni)	CNO treatment	$F_{(1,56)} = 7.25$	>0.05
3B	Vehicle vs CNO/WT vs mutants	6–10	Two-way ANOVA (Bonferroni)	Genotype × CNO treatment	$F_{(3,56)} = 2.74$	0.05
3C	Vehicle vs CNO/WT vs mutants	6–10	Two-way ANOVA (Bonferroni)	Genotype	$F_{(3,55)} = 3.33$	>0.05
3C	Vehicle vs CNO/WT vs mutants	6–10	Two-way ANOVA (Bonferroni)	CNO treatment	$F_{(1,55)} = 8.16$	<0.01
3C	Vehicle vs CNO/WT vs mutants	6–10	Two-way ANOVA (Bonferroni)	Genotype × CNO treatment	$F_{(3,55)} = 4.81$	>0.05
3D	Vehicle vs CNO/WT vs mutants	5–10	Two-way ANOVA (Bonferroni)	Genotype	$F_{(3,50)} = 0.85$	<0.05
3D	Vehicle vs CNO/WT vs mutants	5–10	Two-way ANOVA (Bonferroni)	CNO treatment	$F_{(1,50)} = 7.75$	<0.01
3D	Vehicle vs CNO/WT vs mutants	5–10	Two-way ANOVA (Bonferroni)	Genotype × CNO treatment	$F_{(3,50)} = 1.26$	<0.05
3G	WT vs mutants	6–9	One-way ANOVA (Neuman–Keuls)	Genotype	$F_{(3)} = 8.25$	<0.01
3H	WT vs mutants/pre- vs post-rAAV	6–9	Two-way ANOVA (Bonferroni)	Genotype	$F_{(3,39)} = 2.87$	<0.05
3H	WT vs mutants/pre- vs post-rAAV	6–9	Two-way ANOVA (Bonferroni)	AAV	$F_{(1,39)} = 25$	<0.01
3H	WT vs mutants/pre- vs post-rAAV	6–9	Two-way ANOVA (Bonferroni)	Genotype × AAV	$F_{(3,39)} = 2.87$	<0.05
3I	WT vs mutants	5–9	One-way ANOVA (Neuman–Keuls)	Genotype	$F_{(3)} = 9.00$	<0.01
4A	Control vs hM3Dq-mCherry/CNO doses	8	Two-way ANOVA (Bonferroni)	Nucleofection	$F_{(5,84)} = 8.0$	<0.01
4A	Control vs hM3Dq-mCherry/CNO doses	8	Two-way ANOVA (Bonferroni)	CNO treatment	$F_{(5,84)} = 76$	<0.01
4A	Control vs hM3Dq-mCherry/CNO doses	8	Two-way ANOVA (Bonferroni)	Nucleofection × CNO treatment	$F_{(5,84)} = 6.11$	<0.01
4B	Intracellular signaling inhibitors	4–12	One-way ANOVA (Dunnet)	Inhibitors	$F_{(13)} = 11.66$	<0.01
4C	Mock vs shRNA/vehicle vs CNO	16	Two-way ANOVA (Bonferroni)	Nucleofection	$F_{(5,180)} = 6.46$	<0.01
4C	Mock vs shRNA/vehicle vs CNO	16	Two-way ANOVA (Bonferroni)	CNO treatment	$F_{(1,180)} = 92.15$	<0.01
4C	Mock vs shRNA/vehicle vs CNO	16	Two-way ANOVA (Bonferroni)	Nucleofection × CNO treatment	$F_{(5,180)} = 8.64$	<0.01
4D	Protein/time of treatment	3–4	Two-way ANOVA (Bonferroni)	Protein	$F_{(3,55)} = 2.18$	>0.05
4D	Protein/time of treatment	3–4	Two-way ANOVA (Bonferroni)	Time of treatment	$F_{(5,55)} = 13.67$	<0.01
4D	Protein/time of treatment	3–4	Two-way ANOVA (Bonferroni)	Protein × time of treatment	$F_{(15,55)} = 4.30$	<0.01
4E	Protein/inhibitor	3	Two-way ANOVA (Bonferroni)	Protein	$F_{(3,32)} = 0.92$	>0.05
4E	Protein/inhibitor	3	Two-way ANOVA (Bonferroni)	Inhibitors	$F_{(4,32)} = 16.47$	<0.01
4E	Protein/inhibitor	3	Two-way ANOVA (Bonferroni)	Protein × inhibitors	$F_{(12,32)} = 2.08$	<0.05
5A	Control vs hM3Dq-mCherry/CNO doses	8	Two-way ANOVA (Bonferroni)	Infection	$F_{(5,84)} = 7.07$	<0.01
5A	Control vs hM3Dq-mCherry/CNO doses	8	Two-way ANOVA (Bonferroni)	CNO treatment	$F_{(5,84)} = 33.94$	<0.01
5A	Control vs hM3Dq-mCherry/CNO doses	8	Two-way ANOVA (Bonferroni)	Infection × CNO treatment	$F_{(5,84)} = 4.89$	<0.01
5B	Vehicle vs CNO/vehicle vs inhibitors	8	Two-way ANOVA (Bonferroni)	Inhibitors	$F_{(5,84)} = 0.65$	>0.05
5B	Vehicle vs CNO/vehicle vs inhibitors	8	Two-way ANOVA (Bonferroni)	CNO treatment	$F_{(1,84)} = 3.98$	<0.05
5B	Vehicle vs CNO/vehicle vs inhibitors	8	Two-way ANOVA (Bonferroni)	Inhibitors × CNO treatment	$F_{(5,84)} = 1.11$	>0.05
6A	Vehicle vs CNO	4–5	Unpaired Student's *t* test	CNO treatment	$F_{(4)} = 7.15$	<0.05
6A	CNO vs SP-CNO	4–5	Unpaired Student's *t* test	SP treatment	$F_{(4)} = 6.03$	<0.01
6C	Vehicle vs CNO/CNO vs SP-CNO	5–8	One-way ANOVA (Tukey)	Treatments	$F_{(5)} = 8.14$	<0.01
6D	Vehicle vs CNO/CNO vs SP-CNO	10–11	One-way ANOVA (Tukey)	Treatments	$F_{(5)} = 3.00$	<0.05
7A	Vehicle vs CNO/CNO vs SP-CNO	5–8	One-way ANOVA (Tukey)	Treatments	$F_{(5)} = 6.42$	<0.01
7B	Vehicle vs CNO/CNO vs SP-CNO	5–8	One-way ANOVA (Tukey)	Treatments	$F_{(5)} = 2.82$	<0.05
7C	Vehicle vs CNO/CNO vs SP-CNO	5–8	One-way ANOVA (Tukey)	Treatments	$F_{(5)} = 3.51$	<0.05
8B	D1R vehicle vs CNO	7	One-way ANOVA (Tukey)	Treatments	$F_{(2)} = 7.27$	<0.01
8B	D2R vehicle vs CNO	6–7	One-way ANOVA (Tukey)	Treatments	$F_{(2)} = 11.02$	<0.01

injection at the following coordinates (to bregma): anteroposterior +0.5, lateral ±2.0, and dorsoventral −3.0. Four weeks after surgery, mice were assigned to different experimental groups before starting the pharmacological treatments. Rotarod performance was analyzed along the last 3 d of treatment. Mice were subsequently killed by intracardial perfusion and their brains were excised for immunofluorescence analyses.

Eight-week-old wild-type, D_1R-Cre, D_2R-Cre, and/or D_1R/D_2R-Cre mice were injected either unilaterally into the right brain hemisphere (for assessing rotational behavior) or bilaterally (for assessing motor activity, motor coordination, and sleep–wake pattern) with the Cre-dependent CAG-DIO-hM3Dq-mCherry-rAAV at the aforementioned coordinates. Animals were left untreated for 4 weeks after surgery before the pharmacological treatments and behavioral tests (see below).

Drug administration in vivo

CNO (Santa Cruz Biotechnology) was prepared fresh in saline (0.9% NaCl) just before the experiments and injected intraperitoneally at 1 or 10 mg/kg. SP600125 (2H-dibenzo[cd,g]indazol-6-one) was dissolved in 45% (w/v) β-cyclodextrin (Sigma-Aldrich) and injected intraperitoneally at 15 mg/kg.

Behavioral and electroencephalographic assays

Spontaneous locomotor activity. D_1R-Cre, D_2R-Cre, and D_1R/D_2R-Cre mice and their wild-type littermates were injected bilaterally with CAG-DIO-hM3Dq-mCherry-rAAV as described above. After vector administration, passive retro-reflective markers (B&L Engineering; diameter 7.9 mm, weight < 0.5 g) were attached with acrylic dental cement to the skull

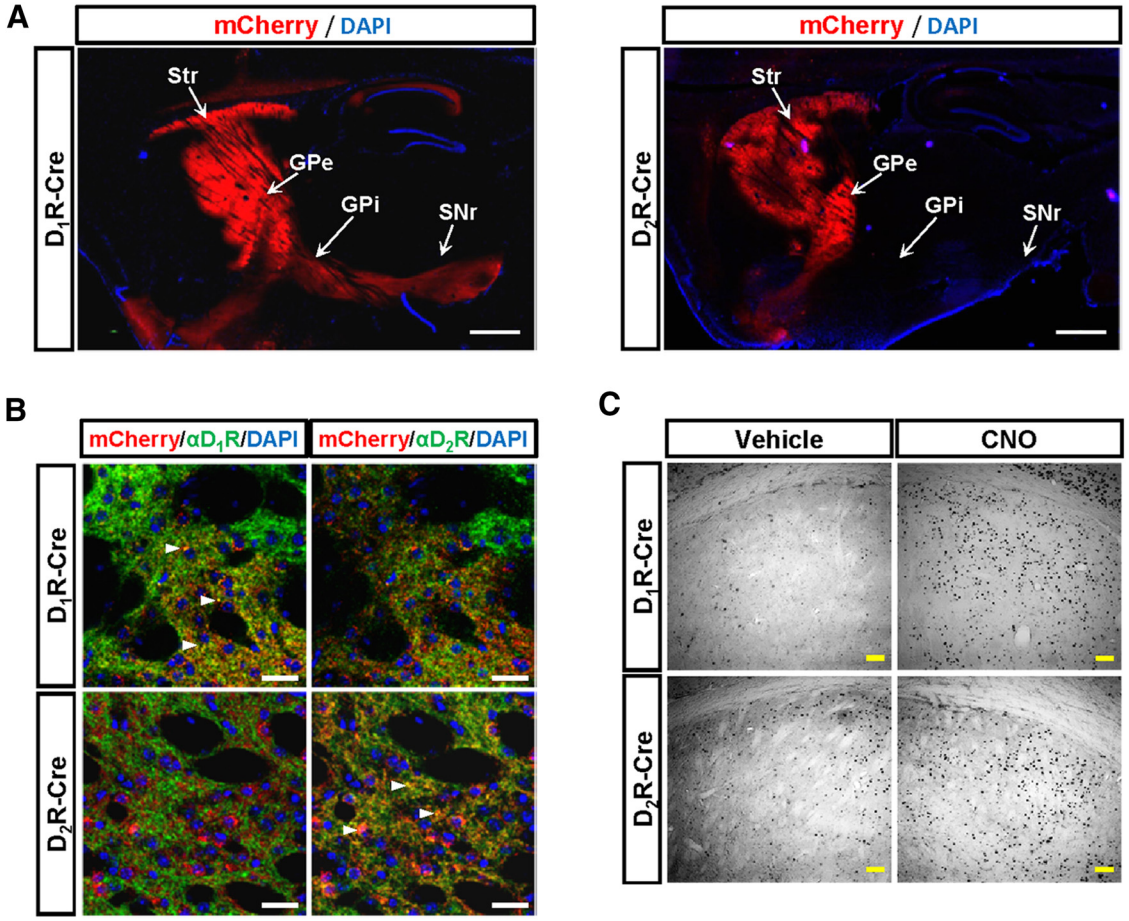

Figure 1. Expression and activity of hM3Dq-mCherry in D_1R-MSNs and D_2R-MSNs *in vivo*. D_1R-Cre and D_2R-Cre mice were injected stereotaxically into the dorsal striatum with CAG-DIO-mCherry-rAAV (***A***) or CAG-DIO-hM3Dq-mCherry-rAAV (***B***, ***C***), and left untreated for 4 weeks. ***A***, Representative images delineating the connectivity from the striatum to output nuclei in D_1R-Cre and D_2R-Cre mice. Str, Striatum; GPe, external globus pallidus; GPi, internal globus pallidus; SNr, substantia nigra pars reticulata. Scale bar, 1 mm. ***B***, Fluorescence colabeling of D_1R/mCherry and D_2R/mCherry shows the specificity of Cre-driven recombination. Examples of cells that are double-positive for D_1R/mCherry or D_2R/mCherry are indicated by arrows. Scale bar, 30 μm. ***C***, Animals subsequently received one single intraperitoneal injection of vehicle or CNO (1 mg/kg) and, after 2 h, were killed for cFos immunohistochemistry. Scale bar, 75 μm.

of each mouse, which was single-housed in its cage. Acquisition (5 Hz frequency) was performed using 3 OptiTrack Flex3 cameras (Natural Point), allowing the continuous recording of the position of each animal during dark and light phases. Acquisition and automated tracking software were from MouvTech. Throughout the study, animals had unrestricted access to water and food and were subjected to a 12 h light/12 h dark cycle. Offline analysis was performed using homemade software developed with Matlab (The MathWorks). Mice were habituated to the home cage for 7 d. They were then injected with vehicle (saline), followed 24 h later by acute CNO (1 mg/kg) and then by chronic CNO (10 mg/kg/d for 14 d). Total locomotor activity in 12 h light/12 h dark cycles was recorded.

Exploration, motor coordination, and spatial recognition. D_1R-Cre, D_2R-Cre, and D_1R/D_2R-Cre mice and their wild-type littermates were injected bilaterally with CAG-DIO-hM3Dq-mCherry-rAAV as described above. They underwent a treatment schedule of 1 d of acute CNO (1 mg/kg) followed by chronic CNO (10 mg/kg/d for 14 d) (or saline vehicle). Exploration analyses were conducted in an automated actimeter (ActiTrack; Panlab; Blázquez et al., 2011) the first day of acute treatment (1 h after injection), as well as after the last day of treatment. Motor coordination (Rotarod test) and spatial recognition (Y-maze test) were evaluated along the last 3 d of treatment before CNO administration to avoid acute drug effects (Blázquez et al., 2011; Pietropaolo et al., 2015).

Sleep–wake pattern. D_1R-Cre, D_2R-Cre, and D_1R/D_2R-Cre mice and their wild-type littermates were injected bilaterally with CAG-DIO-hM3Dq-mCherry-rAAV as described above and implanted a multisite electrode array for electroencephalographic recordings as described previously (Lebreton et al., 2015). Mice underwent two sessions of acute-activation recording, one with vehicle (saline) and another, after 24 h, with CNO (1 mg/kg) plus one session of chronic activation recording after the last day of chronic CNO treatment (10 mg/kg/d for 14 d or saline vehicle). Electrophysiological data were analyzed as described previously (Lebreton et al., 2015).

Rotational behavior. D_1R-Cre and D_2R-Cre mice were injected unilaterally with CAG-DIO-hM3Dq-mCherry-rAAV as described above. Mice were then acutely injected with vehicle (saline) or, after 24 h, with CNO (1 mg/kg); in both cases, animals were tested 1 h later in an open field. Subsequently, animals were injected for 15 d with CNO (10 mg/kg/d) together with SP600125 (15 mg/kg/d) or their respective vehicles. One day after the last treatment, all mice were injected with vehicle and, after 24 h, with CNO (1 mg/kg); in both cases, animals were tested 1 h later in an open field. Ipsilateral movements (complete turning to the right) and contralateral movements (complete turning to the left) were assessed by monitoring manually the total time spent in rotation for 5 min. No rotations were observed in wild-type mice expressing CAG-DIO-hM3Dq-rAAV and injected with vehicle or CNO.

Immunomicroscopy

Coronal free-floating sections (50 μm-thick) were obtained from paraformaldehyde-perfused mouse brains. Samples were incubated with antibodies against dopamine- and cAMP-regulated phosphoprotein of 32 kDa (DARPP-32; 1:1000; BD Biosciences, #611520), NeuN (1:500; Millipore, #MAB377), D_1R (1:500; Frontier Science, #af500), D_2R (1:500; Frontier Science, #af750), choline acetyltransferase (ChaT; 1:1000;

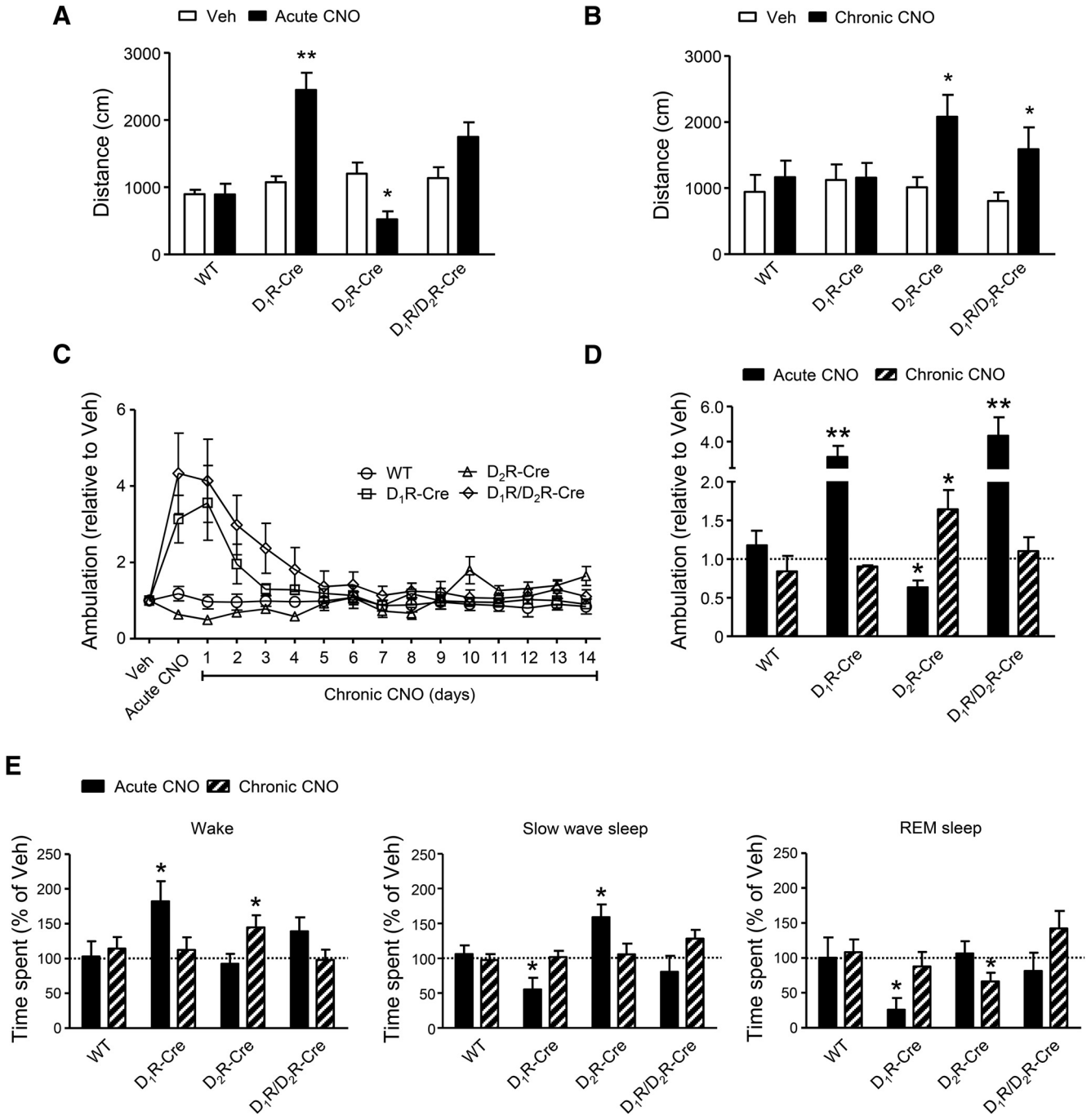

Figure 2. Sustained G_q-protein signaling disrupts the balanced control of behavior exerted by D_1R-MSNs and D_2R-MSNs *in vivo*. Wild-type, D_1R-Cre, D_2R-Cre, and D_1R/D_2R-Cre mice were injected stereotaxically into the dorsal striatum with CAG-DIO-hM3Dq-mCherry-rAAV and left untreated for 4 weeks. ***A***, Animals subsequently received one single intraperitoneal injection of vehicle or CNO (1 mg/kg) and, 1 h later, their ambulation was tested in an open field. ***B***, Animals subsequently received one daily intraperitoneal injection of vehicle or CNO (10 mg/kg) for 14 consecutive days and their ambulation was tested in an open field. ***C***, ***D***, Animals used for continuous ambulatory activity recordings were implanted during surgery light-reflecting devices. They subsequently received one single intraperitoneal injection of vehicle, followed after 24 h by CNO (1 mg/kg; acute CNO) and, after 24 h, one daily intraperitoneal injection of vehicle or CNO (10 mg/kg) for 14 consecutive days (chronic CNO). Total daily ambulations for the 12 h light period (7:00–19:00), expressed as percentage of vehicle treatment, are shown for 16 consecutive days (***C***), as well as for the acute day and the last chronic-treatment day (***D***). ***E***, Animals used for electroencephalographic recordings were implanted during surgery with electrode-miniature array devices. They subsequently underwent 2 sessions of acute-activation electroencephalographic recording, one with vehicle (saline) and another, after 24 h, with CNO (1 mg/kg) plus one session of chronic-activation electroencephalographic recording after the last day of chronic CNO treatment (10 mg/kg/d for 14 consecutive days; or saline vehicle). In each case, animals were subjected to recording for 3 h and sleep–wake changes induced by CNO treatment were expressed as percentage of the respective vehicle treatment. $^*p < 0.05$, $^{**}p < 0.01$ from the corresponding vehicle group (***A***, ***B***) or the wild-type group (***D***, ***E***). See details of statistical analyses in Table 2.

Merck, #AB144P) or cFos (1:2000; Santa Cruz Biotechnology, #SC52), followed by staining with the corresponding Alexa Fluor 488, 594, or 647 antibodies (1:1000; Life Technologies) or with HRP-coupled secondary antibodies plus DAB chromogenic visualization (Vector Laboratories) (Blázquez et al., 2011). Nuclei were visualized with DAPI. Analysis of marker protein immunoreactivity in the dorsal striatum was conducted in a 1-in-10 series per animal (from bregma +1.5 to −0.5 coronal coordinates). For DARPP-32, D_1R, and D_2R, data were calculated as immu-

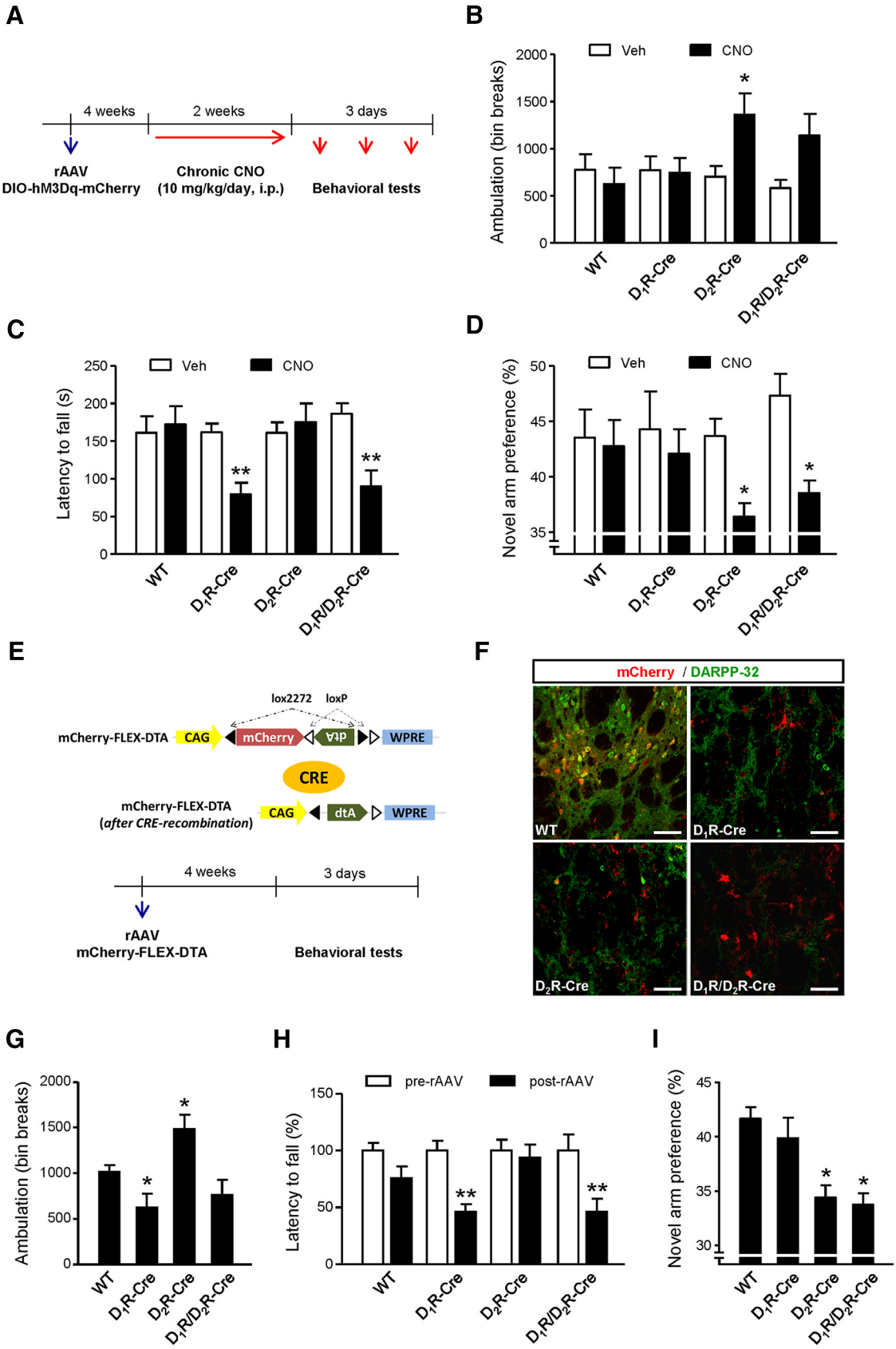

Figure 3. Diphtheria-toxin-mediated ablation of D_1R-MSNs and D_2R-MSNs recapitulates the behavioral phenotype of sustained G_q-protein signaling. ***A–D***, Wild-type, D_1R-Cre, D_2R-Cre, and D_1R/D_2R-Cre mice were injected stereotaxically into the dorsal striatum with CAG-DIO-hM3Dq-mCherry-rAAV and left untreated for 4 weeks. Animals subsequently received one daily intraperitoneal injection of vehicle (saline) or CNO (10 mg/kg) for 2 consecutive weeks. Shown is the scheme of the chronic CNO treatment experiment. The arrows indicate injections (blue, rAAV; red, vehicle/CNO; ***A***). Effect of chronic CNO treatment on ambulation (open field; ***B***), motor coordination (Rotarod; ***C***), and spatial recognition (Y-maze; ***D***). ***E–I***, Wild-type, D_1R-Cre, D_2R-Cre, and D_1R/D_2R-Cre mice were injected stereotaxically into the dorsal striatum with a rAAV encoding mCherry-FLEX-DTA and left untreated for 4 weeks. Scheme of the diphtheria toxin (*Figure legend continues.*)

noreactive area per total cell nuclei and are expressed as a percentage of the control. D_1R and D_2R immunofluorescence was counted simultaneously, so these are shown in the same samples. For NeuN and ChaT, data were calculated as number of positive cells per total cell nuclei and expressed as percentage of the control. Confocal fluorescence images were acquired using TCS-SP2 software and a SP2 AOBS microscope (Leica). Pixel quantification and colocalization were analyzed with ImageJ software.

Western blotting

Western blot analysis was conducted with antibodies raised against phosphorylated ERK (1:1000; Cell Signaling Technology, #9101), total ERK (1:1000; Cell Signaling Technology, #9102), phosphorylated JNK (1:1000; Cell Signaling Technology, #9255), total JNK (1:1000; Cell Signaling Technology, #9252), phosphorylated cJun (1:1000; Cell Signaling Technology, #2361), total cJun (1:1000; Cell Signaling Technology, #9156), phosphorylated PYK2 (1:1000; Cell Signaling Technology, #3291), total PYK2 (1:1000; Cell Signaling Technology, #3480), and β-tubulin III (1:4000; Sigma-Aldrich, #T8660), following standard procedures (Blázquez et al., 2015). Densitometric analysis was performed with Quantity One software (Bio-Rad).

Cell culture

Conditionally immortalized mouse striatal neuroblasts infected with a defective retrovirus transducing the temperature-sensitive A58/U19 large T antigen (Trettel et al., 2000; designated as STHdh cells; provided by Silvia Ginés, University of Barcelona, Spain) were grown at 33°C in DMEM supplemented with 10% fetal bovine serum, 1 mM sodium pyruvate, 2 mM L-glutamine, and 400 μg/ml geneticin (Blázquez et al., 2011). Cells were devoid of mycoplasma contamination.

Primary striatal neurons were obtained from 2-d-old C57BL/6N mice using a papain dissociation system (Worthington). Striata were dissected and cells were seeded on plates precoated with 0.1 mg/ml poly-D-lysine at 200,000 cells/cm^2 in Neurobasal medium supplemented with B27 and Glutamax (Blázquez et al., 2015).

Cell nucleofection and infection

STHdh cells were nucleofected with a construct expressing hM3Dq-mCherry (or mCherry alone as control) under the CAG promoter (see above) using an Amaxa mouse neuron nucleofector kit (Lonza). Two days after nucleofection, cells were treated in 0.5% FBS medium with CNO (or H_2O as vehicle) in the presence of different signaling pathway inhibitors (Table 1). Cells were treated for up to 8 h for cell viability or Western blot assays (Blázquez et al., 2015). In a second set of experiments, the CAG-hM3Dq-mCherry construct was conucleofected with plasmids expressing shRNA directed to *Jnk1*, *Jnk2*, *Jnk3*, or *Pyk2* or a scrambled control (Origene). The extent of silencing induced by the different kinase-directed shRNA, as determined by RT-PCR, ranged between 50% and 80% relative to the scrambled control. In a third set of experiments, STHdh cells were nucleofected with a CAG-DTA construct. Primary neurons were infected at day 2 *in vitro* with a rAAV expressing hM3Dq (or GFP as control) and kept until day 13 *in vitro* for cell viability experiments.

Statistics

Data are presented as mean ± SEM. Statistical comparisons were made by one-way or two-way ANOVA with *post hoc* Bonferroni, Tukey, or Neuman–Keuls test or by unpaired Student's *t* test. The precise statistical analysis made for each figure panel is shown in Table 2. $p < 0.05$ was considered significant.

Results

Sustained G_q-protein signaling disrupts the balanced control of behavior exerted by D_1R-MSNs and D_2R-MSNs *in vivo*

To study the impact of G_q-driven signaling on striatal circuits, we set up an experimental model to manipulate direct-pathway or indirect-pathway MSNs selectively and reliably *in vivo*. For this purpose, we first injected a FLEX (CAG-DIO) rAAV encoding mCherry into the dorsal striatum of D_1R-Cre and D_2R-Cre mice, which allowed delineating the connectivity to output nuclei (Fig. 1*A*). Counting of mCherry-positive cells in D_1R-Cre and D_2R-Cre mice showed that recombination was slightly higher in the former mouse line (63 ± 5% and 40 ± 4% of mCherry-positive cells in D_1R-Cre and D_2R-Cre mice, respectively; $n = 7$ animals per group). We also analyzed mCherry expression in ChaT-positive interneurons and found that our CAG-DIO-rAAV-driven infection procedure generated no detectable recombination in D_1R-Cre mice (0% of ChaT-positive cells infected; $n = 7$ mice) and only a negligible recombination in D_2R-Cre mice (<3% of ChaT-positive cells infected; $n = 7$ mice). Next, a CAG-DIO-rAAV encoding hM3Dq fused to mCherry was injected in the same experimental conditions. The Cre-driven expression of the transgene was achieved selectively in D_1R-MSNs and D_2R-MSNs, as evidenced by D_1R/mCherry and D_2R/mCherry colabeling analyses (Fig. 1*B*). Moreover, the ability of the transgene to trigger neuronal activation was proven by the enhanced cFos immunoreactivity observed in the striata of D_1R-Cre and D_2R-Cre mice (but not wild-type mice) that had been acutely treated with CNO (one single intraperitoneal injection at 1 mg/kg; Alexander et al., 2009; Fig. 1*C*).

In a first experimental paradigm aimed at assessing dorsal striatum functionality, we observed that acute activation of G_q-protein signaling in D_1R-MSNs enhanced exploratory activity in an open field, whereas acute activation in D_2R-MSNs produced the opposite effect (Fig. 2*A*). Strikingly, upon chronic CNO treatment (one daily intraperitoneal injection of CNO at 10 mg/kg for 14 d; Alexander et al., 2009; Chiarlone et al., 2014) the acute G_q-evoked hyperlocomotor reactivity on D_1R-MSNs was abolished and the acute G_q-evoked hypolocomotor reactivity on D_2R-MSNs did not only disappeared, but even turned to an opposite hyperlocomotor reactivity (Fig. 2*B*).

In a second experimental paradigm, the effect of acute and chronic G_q activation in the direct or indirect pathway was monitored using passive retro-reflective markers attached to the head of each mouse expressing hM3Dq-mCherry in D_1R-MSNs or D_2R-MSNs. Singly housed mice were thus continuously tracked in their home cage during 16 consecutive days under vehicle (one single intraperitoneal saline injection), acute CNO (one single intraperitoneal injection at 1 mg/kg the day after) and subsequent chronic CNO (one daily intraperitoneal injection at 10 mg/kg for 14 d). Consistent with the aforementioned open-field data, acute G_q activation in D_1R-MSNs increased continuous ambulatory activity, whereas acute G_q activation in D_2R-MSNs led to the opposite outcome (Fig. 2*C*,*D*). Sustained G_q activation in D_1R-MSNs abolished the acute hyperactivity, whereas sustained G_q activation in D_2R-MSNs turned the acute hypoactivity into hyperactivity (Fig. 2*C*,*D*). These behavioral changes were visible only during light cycle (data not shown for dark cycle). The different response to chronic CNO treatment shown by D_1R/D_2R-Cre mice in Figure 2, *C* and *D*, versus Figure 2*B* most likely reflects the different type of test used, namely locomotor activity in the home cage versus locomotor reactivity in a novel environment. The latter can be subjected to other behavioral compo-

←

(*Figure legend continued.*) expression experiment. The blue arrow indicates rAAV injections (***E***). Fluorescence labeling of mCherry and DARPP-32 shows the effect of Cre-driven recombination in the mCherry-FLEX-DTA animals. Scale bar, 50 μm (***F***). Effect of diphtheria toxin expression on ambulation (open field; ***G***), motor coordination (Rotarod; ***H***), and spatial recognition (Y-maze; ***I***). *$p < 0.05$, **$p < 0.01$ from the corresponding vehicle group (***B***–***D***), wild-type group (***G***, ***I***), or pre-rAAV group (***H***). See details of statistical analyses in Table 2. DTA, Diphtheria toxin fragment A.

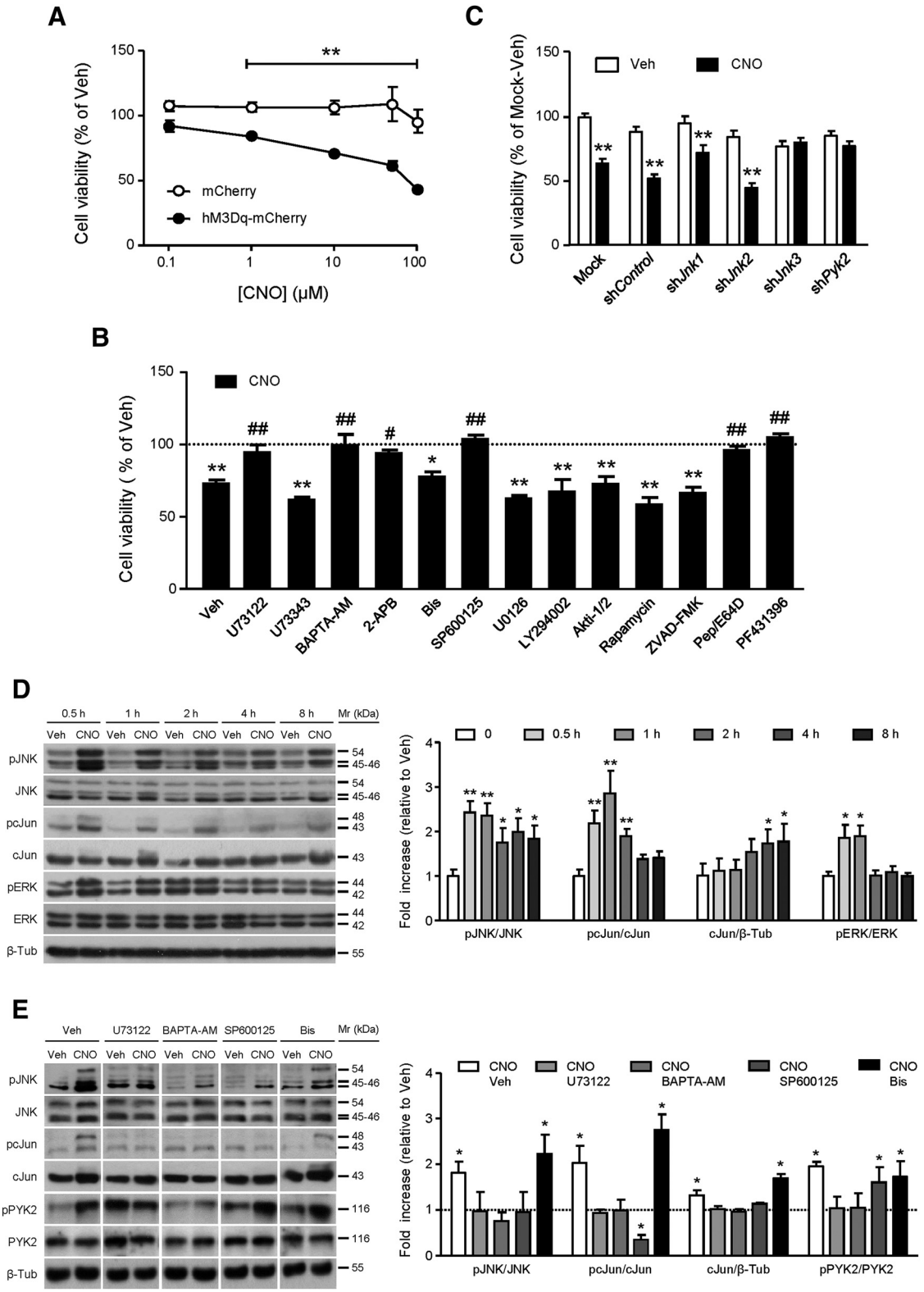

Figure 4. Sustained G_q-protein signaling induces the death of STHdh cells via PLC/Ca^{2+}/PYK2/JNK. STHdh cells were nucleofected with constructs expressing hM3Dq-mCherry or mCherry. ***A***, Cells were incubated for 8 h with vehicle or the indicated doses of CNO. ***B***, Cells were incubated for 8 h with vehicle or 50 μM CNO, together with vehicle or the indicated additions (see experimental details in Table 1). ***C***, Cells were also nucleofected with a nontargeted shRNA, or with shRNAs directed against *Jnk1*, *Jnk2*, *Jnk3*, or *Pyk2* and subsequently incubated for 8 h with vehicle or 50 μM CNO. Relative cell viability is shown in all panels. ***D***, STHdh cells were incubated for the times indicated with vehicle or 50 μM CNO. ***E***, STHdh cells were incubated for 2 h with vehicle or 50 μM CNO, together with vehicle or the indicated additions (see experimental details in Table 1). In ***D*** and ***E***, the representative Western blots with the molecular weight of the protein bands (left) and quantification of optical density values of the protein bands relative to those of loading controls (right) are shown. In ***E*** (left), images from different parts of the same gel or from different gels were grouped. *$p < 0.05$, **$p < 0.01$ from the corresponding vehicle-treated cells. #$p < 0.05$, ##$p < 0.01$ from the corresponding CNO-vehicle-treated cells. See details of statistical analyses in Table 2. Bis, *Bis*indolylmaleimide; Pep, pepstatin A.

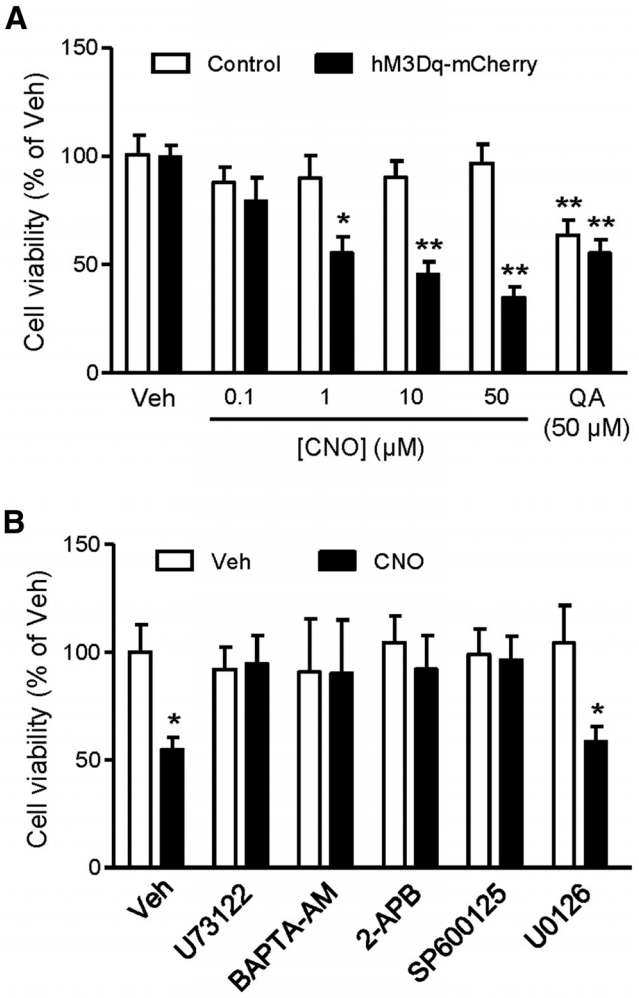

Figure 5. Sustained G_q-protein signaling induces the death of striatal neurons. ***A***, Primary mouse striatal neurons were infected with CAG-hM3Dq-mCherry-rAAV or control CAG-GFP-rAAV at day 2 *in vitro*. At day 13 *in vitro*, they were incubated for 8 h with the indicated doses of CNO. Quinolinic acid (QA) was used as a control neurotoxin to demonstrate a comparable sensitivity to death of CAG-hM3Dq-mCherry-rAAV-infected neurons and CAG-GFP-rAAV-infected neurons. ***B***, Primary mouse striatal neurons were infected with hM3Dq-mCherry-rAAV at day 2 *in vitro*. At day 13 *in vitro*, they were incubated for 8 h with vehicle or 50 μM CNO, together with vehicle or the indicated additions (see experimental details in Table 1). $^*p < 0.05$, $^{**}p < 0.01$ from the corresponding vehicle-treated cells. See details of statistical analyses in Table 2.

nents such as anxiety and risk assessment, which, however, fall beyond the scope of the present study.

A third experimental paradigm was used to evaluate whether the aforementioned behavioral changes in activity were accompanied by actual electroencephalographic changes, specifically in the sleep–wake pattern. Therefore, we found that acute G_q activation in D_1R-MSNs, in concert with hyperactivity, produced an increased amount of wake (Fig. 2*E*, left), as well as a decreased time spent in both slow-wave (Fig. 2*E*, middle) and rapid eye movement (REM) sleep (Fig. 2*E*, right). Acute G_q activation in D_2R-MSNs, in concert with hypoactivity, induced an increased amount of sleep, specifically in the slow-wave phase (Fig. 2*E*, middle). Conversely, sustained G_q activation in D_1R-MSNs abolished, not only the acute hyperactivity, but also the acute wakefulness state (Fig. 2*E*, left), whereas sustained G_q activation in D_2R-MSNs not only induced hyperactivity, but also enhanced the time spent in wake (Fig. 2*E*, left) and reduced the time spent in REM sleep (Fig. 2*E*, right). Spectral analysis of electroencephalograms did not reveal changes in major brain rhythms in the delta, theta, or gamma frequencies during different vigilance states (data not shown).

Collectively, these findings show that direct-pathway and indirect-pathway MSNs can be "turned on" by acute G_q-protein signaling or "turned off" by sustained G_q-protein signaling *in vivo*.

Diphtheria-toxin-mediated ablation of D_1R-MSNs and D_2R-MSNs recapitulates the behavioral phenotype of sustained G_q-protein signaling

To evaluate whether the observed changes elicited by sustained G_q-protein signaling *in vivo* are due to the dysfunction of MSNs, we first analyzed the immunoreactivity of the MSN marker DARPP-32 in D_1R-Cre and D_2R-Cre mice expressing hM3Dq-mCherry in the dorsal striatum. Chronic CNO treatment (10 mg/kg/d for 2 consecutive weeks) decreased DARPP-32 immunoreactivity similarly in D_1R-Cre mice (relative value of CNO vs vehicle: 62 ± 6%; $n = 8$–9 animals per group; $p < 0.01$) and D_2R-Cre mice (relative value of CNO vs vehicle: 70 ± 5%; $n = 7$–8 animals per group; $p < 0.01$). This regime of CNO administration had no significant effect on wild-type mice injected with CAG-DIO-hM3Dq-mCherry-rAAV (relative value of CNO vs vehicle: 96 ± 9; $n = 7$–9 animals per group). Next, we evaluated the behavioral phenotype of D_1R-Cre and D_2R-Cre mice that had been injected stereotaxically into the dorsal striatum with a FLEX-rAAV encoding diphtheria toxin, which is well known to produce cell-population-specific ablation (Kreitzer and Berke, 2011; Durieux et al., 2012; Kim et al., 2014). We selected three behavioral tests that rely at least in part on the dorsal striatum: the open field (to assess exploratory activity), Rotarod (to assess motor coordination), and Y-maze (to assess short-term spatial memory), and compared the phenotype of chronic CNO-treated hM3Dq-mCherry-expressing mice (Fig. 3*A*) with that of diphtheria-toxin-expressing mice (Fig. 3*E*,*F*). Overall, the disrupting effects evoked by the selective expression of diphtheria toxin in D_1R-MSNs or D_2R-MSNs recapitulated very closely the respective changes elicited by sustained G_q signaling in the two MSN populations. Specifically, aside from the exploration assays, in which either chemogenetically or diphtheria toxin-induced dysfunction of D_2R-MSNs enhanced locomotor activity (Fig. 3*B*,*G*), we found that either chemogenetically or diphtheria-toxin-induced dysfunction of D_1R-MSNs impaired motor coordination (Fig. 3*C*,*H*), whereas either chemogenetically or diphtheria-toxin-induced dysfunction of D_2R-MSNs impaired short-term spatial memory (Fig. 3*D*,*I*; no differences in total arm entries were found among the different animal groups tested; data not shown). The lack of motor coordination deficits shown by our D_2R-Cre mice upon chronic CNO administration (Fig. 3*C*), compared with the data reported by Durieux et al. (2012) on mice in which A_{2A}R-expressing neurons had been ablated, could be due to the different experimental conditions used. Therefore, we only analyzed Rotarod performance after training, whereas they found a Rotarod impairment only at the beginning of the training period, after which animals reached the same values as controls. Their D_1R-MSN-ablated mice showed, like ours, a persistent Rotarod impairment also at the end of the training period (Durieux et al. (2012).

Together, these observations suggest that sustained G_q-protein signaling might impair striatal circuits *in vivo* by inducing the inactivation of direct-pathway and indirect-pathway MSNs.

Sustained G_q-protein signaling induces the death of MSNs via a PLC/Ca^{2+}/PYK2/JNK pathway

To analyze the molecular mechanism of G_q-driven action on MSNs, we first used cultures of STHdh mouse striatal neuroblasts, a well established MSN-like cell model (Trettel et al., 2000). Cells were electroporated with a plasmid encoding hM3Dq-mCherry (or only mCherry) and subsequently treated with CNO (or vehicle). Exposure of cells expressing hM3Dq-mCherry (but not mCherry) to CNO decreased viability in a dose-dependent manner (Fig. 4*A*). From these assays, a dose of 50 μM CNO was selected for further experiments aimed at deciphering the signal transduction pathways responsible for G_q-driven cell death (Table 1). The phospholipase C (PLC) inhibitor U73122 (but not its inactive analog U73343), the intracellular Ca^{2+} chelator BAPTA-AM, and the intracellular Ca^{2+}-release inhibitor 2-APB prevented G_q-evoked cell death (Fig. 4*B*), thus supporting the involvement of PLC/Ca^{2+} signaling. In contrast, the general protein kinase C (PKC) inhibitor *bis*indolylmaleimide was ineffective. When assessing potential downstream effectors of PLC/Ca^{2+}, we found that the cJun *N*-terminal kinase (JNK) inhibitor SP600125 prevented G_q-induced cell death, whereas blockade of the extracellular signal-regulated kinase (ERK) cascade (with the MEK inhibitor U0126), phosphatidylinositol 3-kinase (PI3K; with LY294002), Akt (with Akti-1/2), or mammalian target of rapamycin complex 1 (mTORC1; with rapamycin) did not affect G_q action (Fig. 4*B*). G_q-driven STHdh cell death was caspase independent (as evidenced by the lack of effect of the *pan*-caspase inhibitor ZVAD-FMK), but lysosome dependent (as inferred from the preventive effect of the lysosomal-protease/cathepsin inhibitors pepstatin A and E64d; Fig. 4*B*).

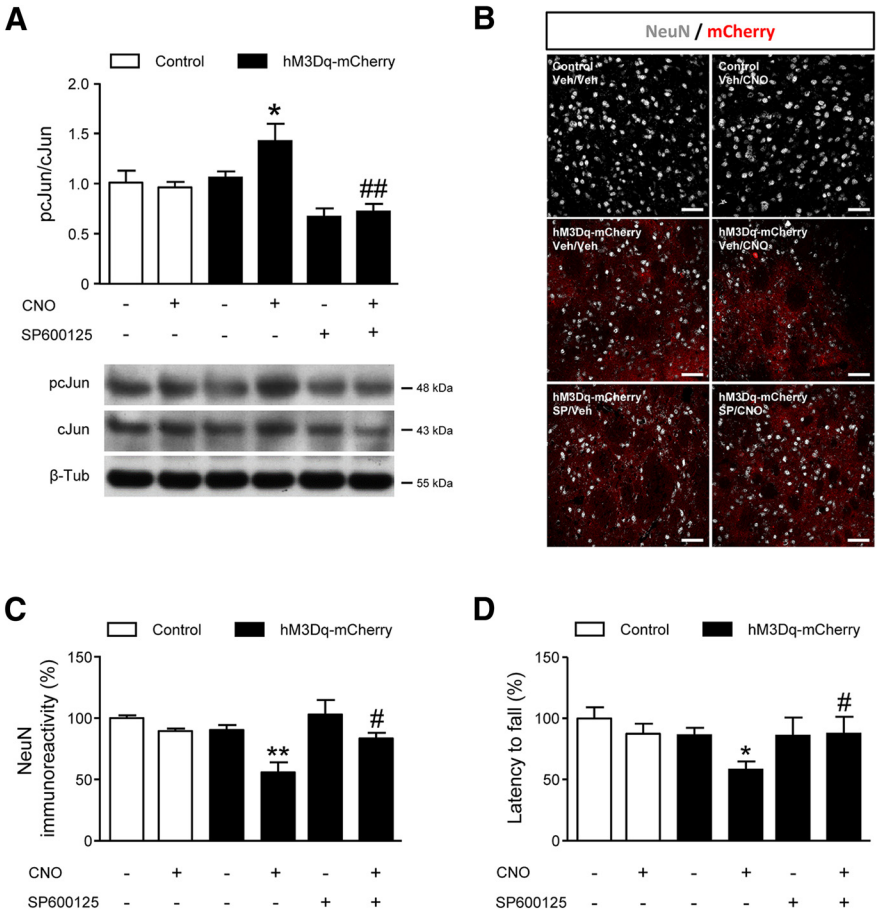

Figure 6. Sustained G_q-protein signaling disrupts the functionality of striatal neurons *in vivo* via JNK. C57BL/6N mice were injected stereotaxically into the dorsal striatum with CAG-hM3Dq-mCherry-rAAV or control CAG-rAAV and left untreated for 4 weeks. ***A***, Animals subsequently received a single intraperitoneal injection of vehicle or CNO (10 mg/kg), together with a single intraperitoneal injection of vehicle or SP600125 (15 mg/kg), and, after 2 h, their dorsal striata were excised for Western blot analysis. Quantification of optical density values of phosphorylated cJun relative to those of the loading control (total cJun; top) and representative Western blots (bottom) are shown. ***B–D***, Animals subsequently received one daily intraperitoneal injection of vehicle or CNO (10 mg/kg), together with one daily intraperitoneal injection of vehicle or SP600125 (15 mg/kg), for 10 consecutive days. Shown are representative images of NeuN immunostaining. Scale bar, 50 μm (***B***). Shown is the quantification of NeuN expression (relative values of NeuN-positive cells; ***C***) and Rotarod test performance (latency to fall; *D*). $^{*}p < 0.05$, $^{**}p < 0.01$ from the corresponding vehicle-vehicle group; $^{\#}p < 0.05$, $^{\#\#}p < 0.01$ from the corresponding CNO-vehicle group. See details of statistical analyses in Table 2.

To further clarify the involvement of the JNK cascade in cell death, we conducted additional experiments in STHdh cells. First, G_q-evoked cell death was prevented by a shRNA targeting JNK3, the most relevant of the three JNK family members in the brain (Fig. 4*C*). Second, Western blot experiments showed that activation of G_q signaling led to a sustained (up to 8 h) phosphorylation (activation) of JNK, which was accompanied by a phosphorylation (activation) and stabilization (increased levels) of its canonical substrate, the transcription factor cJun (Fig. 4*D*). In contrast, the phosphorylation (activation) of ERK, which was used as a control pathway triggered by acute G_q-evoked activation (Girault, 2012), was only transient and returned to basal levels after 2 h of CNO challenge (Fig. 4*D*). Third, consistent with the aforementioned cell death experiments, the sustained G_q-evoked activation of JNK and cJun was PLC/Ca^{2+} dependent (as shown by the preventive effect of U73122 and BAPTA-AM) and PKC independent (as shown by the lack of effect of *bis*indolylmaleimide; Fig. 4*E*).

We next investigated the link between Ca^{2+} and JNK. Proline-rich tyrosine kinase 2 (PYK2) is a cytoplasmic nonreceptor tyrosine kinase enriched in neurons that controls various neurobiological functions and that, by acting as a Ca^{2+} effector, can activate mitogen-activated protein kinase cascades (Girault et al., 1999). Therefore, we investigated whether PYK2 was involved in our experimental setting. The G_q-evoked death of STHdh cells was prevented by the dual PYK2/focal adhesion kinase inhibitor PF431396 (Fig. 4*B*), as well as by a *Pyk2*-directed shRNA (Fig. 4*C*). Likewise, activation of G_q signaling led to the phosphorylation (activation) of PYK2 and this effect was prevented by U73122 and BAPTA-AM, but not by SP600125 (Fig. 3*E*), thus supporting that PYK2 is downstream of PLC/Ca^{2+} and upstream of JNK.

We subsequently investigated whether the G_q-triggered effects observed in STHdh cells could be extrapolated to a more physiological experimental model as primary striatal neurons. Indeed,

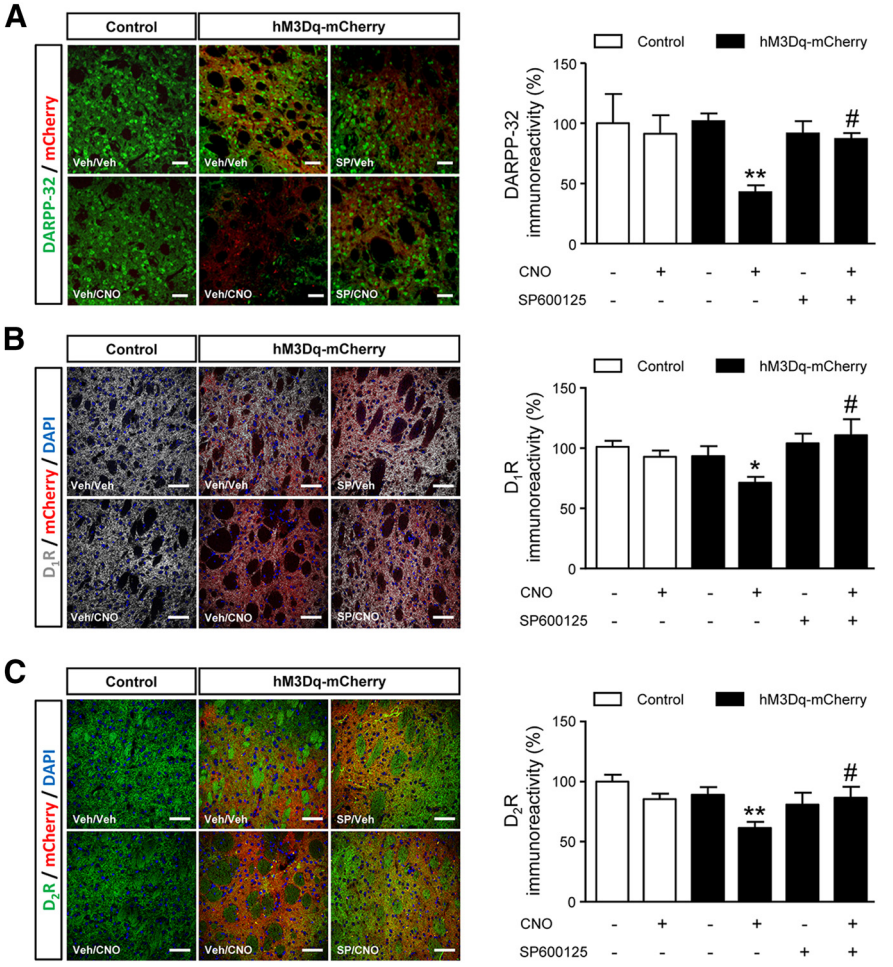

Figure 7. Sustained G_q-protein signaling induces the loss of MSNs *in vivo* via JNK. C57BL/6N mice were injected stereotaxically into the dorsal striatum with CAG-hM3Dq-mCherry-rAAV or control CAG-rAAV, and left untreated for 4 weeks. Animals subsequently received one daily intraperitoneal injection of vehicle or CNO (10 mg/kg), together with one daily intraperitoneal injection of vehicle or SP600125 (15 mg/kg), for 10 consecutive days. ***A***, DARPP-32 expression (relative values of DARPP-32 immunoreactivity). ***B***, D_1R expression (relative values of D_1R immunoreactivity). ***C***, D_2R expression (relative values of D_2R immunoreactivity). Representative images are shown in all panels. Scale bar, 50 μm. $^*p < 0.05$, $^{**}p < 0.01$ from the corresponding vehicle/vehicle group; $^{\#}p < 0.05$ from the corresponding CNO/vehicle group. See details of statistical analyses in Table 2.

activation of G_q signaling upon challenge of hM3Dq-mCherry-expressing primary mouse striatal neurons to CNO also led to a PLC/Ca^{2+}/JNK-dependent, ERK-independent cell death process (Fig. 5*A*,*B*).

In sum, these data show that sustained G_q-protein activation signals neuronal cell death via a PLC/Ca^{2+}/PYK2/JNK-dependent pathway.

Sustained G_q-protein signaling disrupts the functionality of D_1R-MSNs and D_2R-MSNs *in vivo* via JNK

To evaluate the functional relevance of JNK *in vivo*, we first injected C57BL/6N mice stereotaxically into the dorsal striatum with a rAAV encoding hM3Dq-mCherry (or control rAAV). The transgene was driven by the CAG promoter to allow its expression in all MSNs. In agreement with our aforementioned cell culture observations, engagement of G_q signaling (one single intraperitoneal injection of CNO at 10 mg/kg in hM3Dq-mCherry-expressing mice) triggered striatal JNK activation *in vivo*, as determined by the SP600125-sensitive phosphorylation (activation) of cJun (Fig. 6*A*; we were unable to obtain technically reliable Western blots from mouse striatal extracts with commercial anti-pJNK antibodies). Furthermore, after sustained G_q signaling (one daily intraperitoneal injection of CNO at 10 mg/kg for 10 d), we found a loss of MSNs, as determined by the reduction of the neuronal marker NeuN (Fig. 6*B*,*C*) and the MSN marker DARPP-32 (Fig. 7*A*). This loss of MSNs was equally evident in the D_1R-MSN population (Fig. 7*B*) and the D_2R-MSN population (Fig. 7*C*). Moreover, these alterations in neuronal markers were accompanied by a deficit in the Rotarod test (Fig. 6*D*), a well established behavioral readout of the dorsal striatum. Remarkably, these G_q-evoked effects were prevented by pharmacological blockade of JNK (Figs. 6*B–D*, 7*A–C*) and were not simply caused by the viral expression of a novel receptor or by an off-target action of CNO (either hM3Dq-mCherry expression in the absence of CNO or treatment of control rAAV-infected animals with CNO was ineffective; Figs. 6*A–D*, 7*A–C*).

Finally, we assessed whether JNK-driven signaling affects either the direct pathway or the indirect pathway separately by monitoring a clear-cut behavioral task as contraversive movements (Tecuapetla et al., 2014). Selective acute unilateral activation of G_q signaling in D_1R-MSNs or D_2R-MSNs induced contralateral or ipsilateral movements, respectively (Fig. 8*A*). This acute effect was abrogated in those animals that had been chronically treated with CNO (Fig. 8*B*). In turn, this impairing effect of chronic CNO treatment on contralateral/D_1R-MSN-dependent movements (Fig. 8*B*, left) and ipsilateral/D_2R-MSN-dependent movements (Fig. 8*B*, right) was rescued by the coadministration of a JNK inhibitor to the animals.

Collectively, these data show that JNK mediates the inactivation of MSNs and the disruption of striatal circuits evoked by sustained G_q-protein signaling *in vivo*.

Discussion

Here, we manipulated MSNs selectively by means of the DREADD technology to unveil how G_q-protein-evoked signaling affects neuronal functionality. A DREADDi approach was used previously to study the effects of the selective inhibition of D_1R-MSNs or D_2R-MSNs in the rat dorsomedial striatum by expressing hM4Di in a herpes virus vector with promoter elements for dynorphin or enkephalin, respectively (Ferguson et al., 2011). CNO administration did not change acute locomotor responses to amphetamine, but altered behavioral plasticity associated with repeated drug treatment (Ferguson et al., 2011). A similar approach found that the hM4Di-evoked inhibition of D_2R-MSNs in the mouse nucleus accumbens enhanced the motivation to obtain cocaine (Bock et al., 2013). Collectively, these and other related studies demonstrate that chemogenetic manipulation of MSNs with DREADDs (Farrell et al., 2013; Ferguson et al., 2013), DREADDi (Ferguson et al., 2011; Bock et al., 2013; Ferguson et

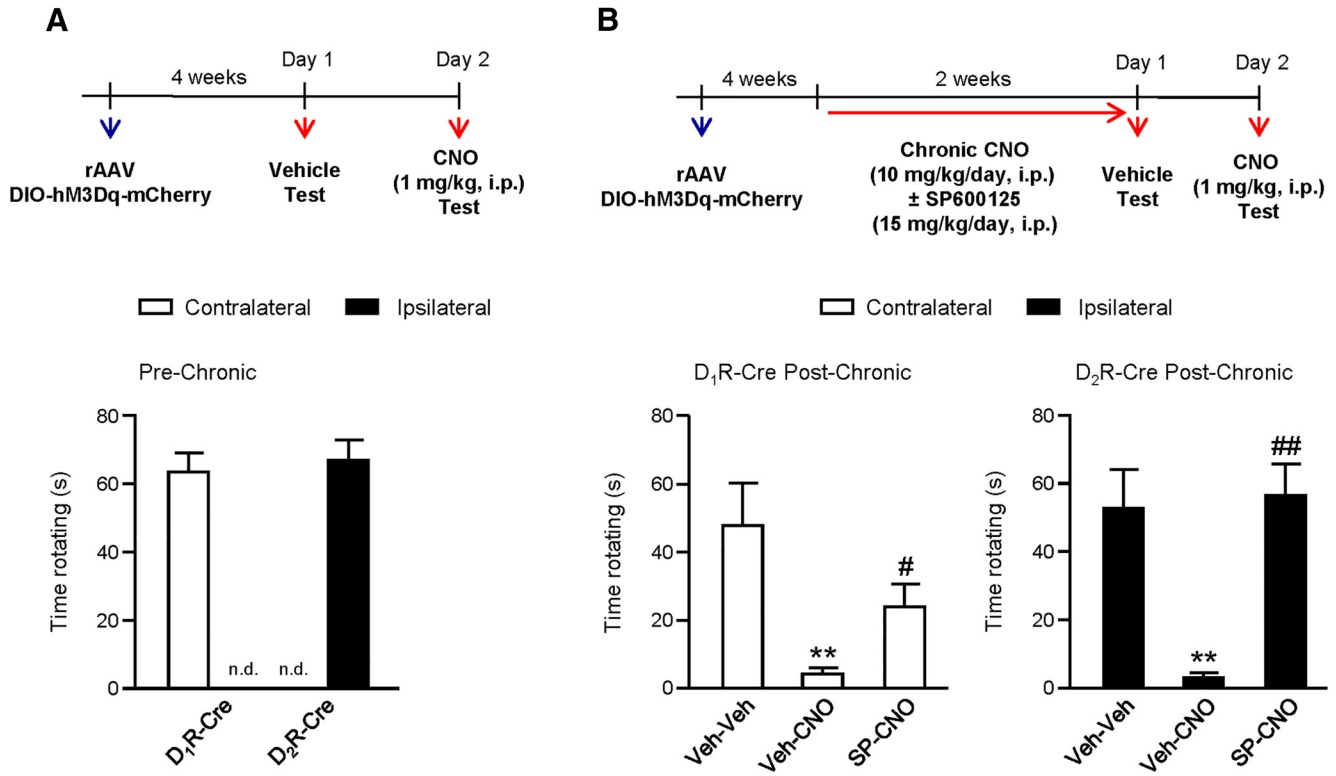

Figure 8. Sustained G_q-protein signaling disrupts the functionality of D_1R-MSNs and D_2R-MSNs *in vivo* via JNK. Wild-type, D_1R-Cre, and D_2R-Cre mice received a unilateral injection into the right dorsal striatum of CAG-DIO-hM3Dq-mCherry-rAAV and were left untreated for 4 weeks. ***A***, Animals subsequently received a single injection of vehicle or, after 24 h, of CNO (1 mg/kg); in both cases, animals were tested 1 h later in an open field. A scheme of this acute CNO treatment experiment is shown on top. The arrows indicate injections (blue, rAAV; red, vehicle/CNO). ***B***, Animals subsequently received one daily intraperitoneal injection of vehicle or CNO (10 mg/kg), together with one daily intraperitoneal injection of vehicle or SP600125 (15 mg/kg), for 15 consecutive days. One day after the last treatment, all mice were injected with vehicle and, after 24 h, with CNO (1 mg/kg); in both cases, animals were tested 1 h later in an open field (left, D_1R-Cre mice; right, D_2R-Cre mice). A scheme of this chronic CNO treatment experiment is shown at the top. The arrows indicate injections (blue, rAAV; red, vehicle/CNO). Ipsilateral and contralateral movements were monitored for 5 minutes. $^{**}p < 0.01$ from the corresponding vehicle/vehicle group. $\#p < 0.05$, $\#\#p < 0.01$ from the corresponding vehicle-CNO group. See details of statistical analyses in Table 2. n.d., Nondetectable.

al., 2013) or DREADDq (the present study) is a viable tool to assess the impact of specific G-protein-mediated signals on the conceptually proposed opposing roles of the direct and indirect striatal pathways. Moreover, the lack of effect of MSN inhibition (via DREADDi) on acute locomotor responses (Ferguson et al., 2011) compared with the remarkable effects of MSN activation via DREADDs (Ferguson et al., 2013) or DREADDq (the present study) points to a hierarchical subordination of inhibitory to stimulatory metabotropic pathways in simple behavioral tasks. Likewise, G_q, G_s, and G_i-coupled DREADD-mediated manipulation of the circadian pacemaker in the mouse suprachiasmatic nucleus showed a prominent role of the G_q axis over G_i (and G_s) signaling in controlling circadian rhythms (Brancaccio et al., 2013). In contrast, significant—and opposing—effects of G_q and G_i signaling per se were found upon the chemogenetic manipulation of, for example, mouse agouti-related protein-expressing neurons (Krashes et al., 2011) and calcitonin-gene-related peptide-expressing neurons (Carter et al., 2013) in the control of feeding behavior. Therefore, it is conceivable that the actual relative strength of G_q, G_s, and G_i signals to control neural activity varies significantly among different brain regions and biological processes *in vivo*.

The precise metabotropic mechanisms involved in the control of the integrity and function of MSNs are not fully understood. A large body of evidence supports that cAMP-dependent cascades are highly relevant and, in fact, both DREADDs and DREADDi alter neuronal activity and plasticity in striatal circuits through changes in cAMP production (Ferguson et al., 2011; Bock et al., 2013; Farrell et al., 2013; Ferguson et al., 2013). Activation of G_{olf}-coupled D_1R in direct-pathway MSNs engages multiple signaling pathways, such as protein kinase A, ERK, and CREB, by increasing cAMP production, whereas activation of G_i-coupled D_2R in indirect-pathway MSNs leads to downregulation of these cascades (Girault, 2012; Cahill et al., 2014). Other G_s-coupled receptors (e.g., adenosine A_{2A} receptors, which are mostly located in striatopallidal MSNs) and G_i-coupled receptors (e.g., cannabinoid CB_1 receptors, which are highly enriched in the terminals of both striatonigral and striatopallidal MSNs) make a major contribution as well to tuning the functioning of basal ganglia circuits via cAMP and other related intracellular signals (Kreitzer, 2009; Girault, 2012).

The class I metabotropic glutamate receptors $mGlu_1$ and $mGlu_5$ are the most relevant group of striatal G_q-coupled receptors. Although activation of the ERK pathway in the striatum can be readily achieved by D_1R and ionotropic (NMDA) glutamate receptors, $mGlu_{1/5}$ receptors also activate ERK through Ca^{2+} release from intracellular stores in synergy with D_1R, thereby participating, for example, in drug-induced behavioral plasticity (Girault, 2012). However, here, by manipulating G_q-evoked activity selectively in MSNs, we unveil that JNK, rather than ERK or other signaling pathways such as PKC and PI3K/Akt/mTORC1, is the key functional effector of the G_q/PLC/Ca^{2+} axis (Fig. 9*A*,*B*). Glutamate has been shown to stimulate JNK in striatal neurons (Schwarzschild et al., 1997) and to cooperate with dopa-

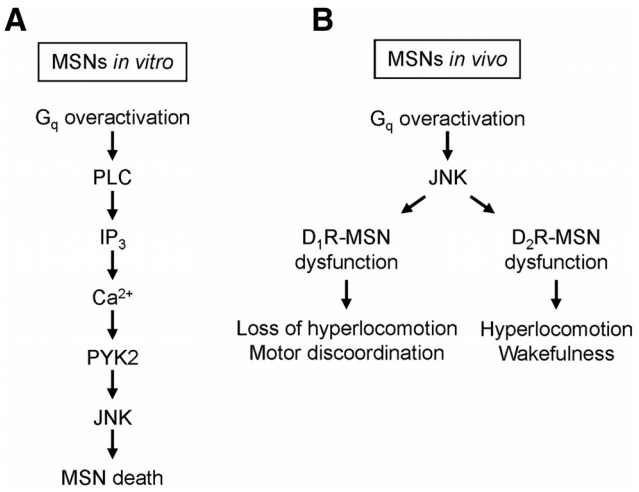

Figure 9. Proposed mechanism of action and impact of sustained G_q-protein signaling on striatal circuitry. ***A***, G_q-protein-coupled signaling upon hM3Dq overactivation in MSNs *in vitro* induces cell death via a PLC/Ca^{2+}/PYK2/JNK pathway. ***B***, G_q-protein-coupled signaling upon hM3Dq overactivation in MSNs *in vivo* induces neuronal dysfuction via JNK, which translates into loss of hyperlocomotion and motor discoordination (upon D1R-MSN dysfunction) or into hyperlocomotion and wakefulness (upon D2R-MSN dysfunction).

minergic signaling (mostly via D_1R) to induce MSN excitotoxicity (McLaughlin et al., 1998; Tang et al., 2007; Paoletti et al., 2008; Chen et al., 2013). Moreover, cocaine (Go et al., 2010) and methamphetamine (Jayanthi et al., 2002) administration, by overstimulating D_1R-mediated dopaminergic signaling, induces MSN death and striatal damage at least in part via JNK, an effect that is favored by activation of class I mGlu receptors (Jayanthi et al., 2002; Go et al., 2010). Therefore, our data align well with prior evidence and strongly support the notion that the JNK cascade plays a pivotal converging role in mediating the malfunctioning of striatal circuits that occurs after overactivation of glutamatergic and dopaminergic transmission (Chen et al., 2013; Cahill et al., 2014). Specifically regarding Huntington's disease, the involvement of JNK in mutant huntingtin-mediated striatal neurotoxicity is supported by a number of *in vitro* and *in vivo* studies (Apostol et al., 2008; Perrin et al., 2009; Taylor et al., 2013). Although we are aware that the primary mechanisms underlying the sustained G_q-protein-induced toxicity of MSNs and the DTA-induced toxicity of MSNs are conceivably distinct, pilot experiments conducted in our STHdh cell cultures show that DTA-induced death also seems to be JNK dependent, as shown by the preventive effect of SP600125 (authors' unpublished observations).

PYK2 was originally characterized as a Ca^{2+}-dependent protein kinase that can link elevations of cytosolic free Ca^{2+} concentration (Yu et al., 1996) with JNK activation upon different triggers (Dikic et al., 1996; Tokiwa et al., 1996). PYK2 is highly responsive to neuronal activity. Upon depolarization, it autophosphorylates on tyrosine residues, clusters on postsynaptic densities, and exposes an SH2-binding domain that recruits Src family kinases, thereby activating various signaling pathways (Girault et al., 1999; Bartos et al., 2010). Therefore, PYK2 may connect neuronal activity/plasticity with processes such as neuronal survival and neurite outgrowth/retraction (Girault et al., 1999; Ivankovic-Dikic et al., 2000; Kinoshita et al., 2014). In addition, PYK2 is activated in the rat hippocampus after brain ischemia and kainate-induced convulsions (Tian et al., 2000), which suggests a role for the kinase in the effects of these insults. Therefore, our present findings extend this evidence and specifically show that PYK2 is a novel mediator of G_q/Ca^{2+}-driven striatal dysfunction (Fig. 9*A*).

In conclusion, this work sheds new light onto how metabotropic signals control neuronal integrity and functionality. It also supports that the sustained DREADDq-evoked modulation of the direct versus indirect pathway may be adopted as a new tool to understand physiopathological alterations occurring in basal-ganglia-related diseases such as Huntington's disease, Parkinson's disease, and L-DOPA-induced dyskinesia. For example, regarding Huntington's disease, the impairment of indirect-pathway circuitry evoked by sustained G_q/JNK signaling seems to recapitulate the dyskinesia/hyperkinesia, as well as the insomnia/reduced REM sleep occurring from early stages of the disease, whereas the impairment of direct-pathway circuitry evoked by sustained G_q/JNK signaling seems to recapitulate the bradykinesia/parkinsonism occurring at later stages of the disease (Fig. 9*B*; Walker, 2007; Arnulf et al., 2008). Whether G_q/JNK signaling affects, not only motor behavior, but also other prominent striatal functions such as cognition and motivation may be the subject of future studies.

References

Alexander GM, Rogan SC, Abbas AI, Armbruster BN, Pei Y, Allen JA, Nonneman RJ, Hartmann J, Moy SS, Nicolelis MA, McNamara JO, Roth BL (2009) Remote control of neuronal activity in transgenic mice expressing evolved G protein-coupled receptors. Neuron 63:27–39. CrossRef Medline

Apostol BL, Simmons DA, Zuccato C, Illes K, Pallos J, Casale M, Conforti P, Ramos C, Roarke M, Kathuria S, Cattaneo E, Marsh JL, Thompson LM (2008) CEP-1347 reduces mutant huntingtin-associated neurotoxicity and restores BDNF levels in R6/2 mice. Mol Cell Neurosci 39:8–20. CrossRef Medline

Armbruster BN, Li X, Pausch MH, Herlitze S, Roth BL (2007) Evolving the lock to fit the key to create a family of G protein-coupled receptors potently activated by an inert ligand. Proc Natl Acad Sci U S A 104:5163–5168. CrossRef Medline

Arnulf I, Nielsen J, Lohmann E, Schieffer J, Wild E, Jennum P, Konofal E, Walker M, Oudiette D, Tabrizi S, Durr A (2008) Rapid eye movement sleep disturbances in Huntington disease. Arch Neurol 65:482–488. CrossRef Medline

Bartos JA, Ulrich JD, Li H, Beazely MA, Chen Y, Macdonald JF, Hell JW (2010) Postsynaptic clustering and activation of Pyk2 by PSD-95. J Neurosci 30:449–463. CrossRef Medline

Blázquez C et al. (2011) Loss of striatal type 1 cannabinoid receptors is a key pathogenic factor in Huntington's disease. Brain 134:119–136. CrossRef Medline

Blázquez C, Chiarlone A, Bellocchio L, Resel E, Pruunsild P, García-Rincón D, Sendtner M, Timmusk T, Lutz B, Galve-Roperh I, Guzmán M (2015) The CB_1 cannabinoid receptor signals striatal neuroprotection via a PI3K/Akt/mTORC1/BDNF pathway. Cell Death Differ 22:1618–1629. CrossRef Medline

Bock R, Shin JH, Kaplan AR, Dobi A, Markey E, Kramer PF, Gremel CM, Christensen CH, Adrover MF, Alvarez VA (2013) Strengthening the accumbal indirect pathway promotes resilience to compulsive cocaine use. Nat Neurosci 16:632–638. CrossRef Medline

Brancaccio M, Maywood ES, Chesham JE, Loudon AS, Hastings MH (2013) A G_q-Ca^{2+} axis controls circuit-level encoding of circadian time in the suprachiasmatic nucleus. Neuron 78:714–728. CrossRef Medline

Cahill E, Salery M, Vanhoutte P, Caboche J (2014) Convergence of dopamine and glutamate signaling onto striatal ERK activation in response to drugs of abuse. Front Pharmacol 4:172. CrossRef Medline

Carter ME, Soden ME, Zweifel LS, Palmiter RD (2013) Genetic identification of a neural circuit that suppresses appetite. Nature 503:111–114. CrossRef Medline

Chen JY, Wang EA, Cepeda C, Levine MS (2013) Dopamine imbalance in Huntington's disease: a mechanism for the lack of behavioral flexibility. Front Neurosci 7:114. CrossRef Medline

Chiarlone A, Bellocchio L, Blázquez C, Resel E, Soria-Gómez E, Cannich A,

Ferrero JJ, Sagredo O, Benito C, Romero J, Sánchez-Prieto J, Lutz B, Fernández-Ruiz J, Galve-Roperh I, Guzmán M (2014) A restricted population of CB_1 cannabinoid receptors with neuroprotective activity. Proc Natl Acad Sci U S A 111:8257–8262. CrossRef Medline

Conn PJ, Battaglia G, Marino MJ, Nicoletti F (2005) Metabotropic glutamate receptors in the basal ganglia motor circuit. Nat Rev Neurosci 6:787–798. CrossRef Medline

Dikic I, Tokiwa G, Lev S, Courtneidge SA, Schlessinger J (1996) A role for Pyk2 and Src in linking G-protein-coupled receptors with MAP kinase activation. Nature 383:547–550. CrossRef Medline

Durieux PF, Schiffmann SN, de Kerchove d'Exaerde A (2012) Differential regulation of motor control and response to dopaminergic drugs by D1R and D2R neurons in distinct dorsal striatum subregions. EMBO J 31:640–653. CrossRef Medline

Farrell MS, Pei Y, Wan Y, Yadav PN, Daigle TL, Urban DJ, Lee HM, Sciaky N, Simmons A, Nonneman RJ, Huang XP, Hufeisen SJ, Guettier JM, Moy SS, Wess J, Caron MG, Calakos N, Roth BL (2013) A Gαs DREADD mouse for selective modulation of cAMP production in striatopallidal neurons. Neuropsychopharmacology 38:854–862. CrossRef Medline

Ferguson SM, Eskenazi D, Ishikawa M, Wanat MJ, Phillips PE, Dong Y, Roth BL, Neumaier JF (2011) Transient neuronal inhibition reveals opposing roles of indirect and direct pathways in sensitization. Nat Neurosci 14:22–24. CrossRef Medline

Ferguson SM, Phillips PE, Roth BL, Wess J, Neumaier JF (2013) Direct-pathway striatal neurons regulate the retention of decision-making strategies. J Neurosci 33:11668–11676. CrossRef Medline

Freeze BS, Kravitz AV, Hammack N, Berke JD, Kreitzer AC (2013) Control of basal ganglia output by direct and indirect pathway projection neurons. J Neurosci 33:18531–18539. CrossRef Medline

Girault JA (2012) Integrating neurotransmission in striatal medium spiny neurons. Adv Exp Med Biol 970:407–429. CrossRef Medline

Girault JA, Costa A, Derkinderen P, Studler JM, Toutant M (1999) FAK and PYK2/CAKβ in the nervous system: a link between neuronal activity, plasticity and survival? Trends Neurosci 22:257–263. CrossRef Medline

Go BS, Ahn SM, Shim I, Choe ES (2010) Activation of c-Jun N-terminal kinase is required for the regulation of endoplasmic reticulum stress response in the rat dorsal striatum following repeated cocaine administration. Neuropharmacology 59:100–106. CrossRef Medline

Ivankovic-Dikic I, Grönroos E, Blaukat A, Barth BU, Dikic I (2000) Pyk2 and FAK regulate neurite outgrowth induced by growth factors and integrins. Nat Cell Biol 2:574–581. CrossRef Medline

Jayanthi S, McCoy MT, Ladenheim B, Cadet JL (2002) Methamphetamine causes coordinate regulation of Src, Cas, Crk, and the Jun N-terminal kinase-Jun pathway. Mol Pharmacol 61:1124–1131. CrossRef Medline

Jennings JH, Stuber GD (2014) Tools for resolving functional activity and connectivity within intact neural circuits. Curr Biol 24:R41–R50. CrossRef Medline

Kim HA, Jiang L, Madsen H, Parish CL, Massalas J, Smardencas A, O'Leary C, Gantois I, O'Tuathaigh C, Waddington JL, Ehrlich ME, Lawrence AJ, Drago J (2014) Resolving pathobiological mechanisms relating to Huntington disease: gait, balance, and involuntary movements in mice with targeted ablation of striatal D1 dopamine receptor cells. Neurobiol Dis 62:323–337. CrossRef Medline

Kinoshita Y, Hunter RG, Gray JD, Mesias R, McEwen BS, Benson DL, Kohtz DS (2014) Role for NUP62 depletion and PYK2 redistribution in dendritic retraction resulting from chronic stress. Proc Natl Acad Sci U S A 111:16130–16135. CrossRef Medline

Krashes MJ, Koda S, Ye C, Rogan SC, Adams AC, Cusher DS, Maratos-Flier E, Roth BL, Lowell BB (2011) Rapid, reversible activation of AgRP neurons drives feeding behavior in mice. J Clin Invest 121:1424–1428. CrossRef Medline

Kreitzer AC (2009) Physiology and pharmacology of striatal neurons. Annu Rev Neurosci 32:127–147. CrossRef Medline

Kreitzer AC, Berke JD (2011) Investigating striatal function through cell-type-specific manipulations. Neuroscience 198:19–26. CrossRef Medline

Lebreton F, Cayzac S, Pietropaolo S, Jeantet Y, Cho YH (2015) Sleep physiology alterations precede plethoric phenotypic changes in R6/1 Huntington's disease mice. PLoS One 10:e0126972. CrossRef Medline

Lee HM, Giguere PM, Roth BL (2014) DREADDs: novel tools for drug discovery and development. Drug Discov Today 19:469–473. CrossRef Medline

McLaughlin BA, Nelson D, Erecińska M, Chesselet MF (1998) Toxicity of dopamine to striatal neurons in vitro and potentiation of cell death by a mitochondrial inhibitor. J Neurochem 70:2406–2415. Medline

Monory K et al. (2006) The endocannabinoid system controls key epileptogenic circuits in the hippocampus. Neuron 51:455–466. CrossRef Medline

Monory K, Blaudzun H, Massa F, Kaiser N, Lemberger T, Schütz G, Wotjak CT, Lutz B, Marsicano G (2007) Genetic dissection of behavioural and autonomic effects of delta-9-tetrahydrocannabinol in mice. PLoS Biol 5:e269. CrossRef Medline

Nelson AB, Kreitzer AC (2014) Reassessing models of basal ganglia function and dysfunction. Annu Rev Neurosci 37:117–135. CrossRef Medline

Paoletti P, Vila I, Rifé M, Lizcano JM, Alberch J, Ginés S (2008) Dopaminergic and glutamatergic signaling crosstalk in Huntington's disease neurodegeneration: the role of p25/cyclin-dependent kinase 5. J Neurosci 28:10090–10101. CrossRef Medline

Perrin V, Dufour N, Raoul C, Hassig R, Brouillet E, Aebischer P, Luthi-Carter R, Déglon N (2009) Implication of the JNK pathway in a rat model of Huntington's disease. Exp Neurol 215:191–200. CrossRef Medline

Pietropaolo S, Bellocchio L, Ruiz-Calvo A, Cabanas M, Du Z, Guzmán M, Garret M, Cho YH (2015) Chronic cannabinoid receptor stimulation selectively prevents motor impairments in a mouse model of Huntington's disease. Neuropharmacology 89:368–374. CrossRef Medline

Ribeiro FM, Pires RG, Ferguson SS (2011) Huntington's disease and Group I metabotropic glutamate receptors. Mol Neurobiol 43:1–11. CrossRef Medline

Schwarzschild MA, Cole RL, Hyman SE (1997) Glutamate, but not dopamine, stimulates stress-activated protein kinase and AP-1-mediated transcription in striatal neurons. J Neurosci 17:3455–3466. Medline

Tang TS, Chen X, Liu J, Bezprozvanny I (2007) Dopaminergic signaling and striatal neurodegeneration in Huntington's disease. J Neurosci 27:7899–7910. CrossRef Medline

Taylor DM, Moser R, Régulier E, Breuillaud L, Dixon M, Beesen AA, Elliston L, Silva Santos Mde F, Kim J, Jones L, Goldstein DR, Ferrante RJ, Luthi-Carter R (2013) MAP kinase phosphatase 1 (MKP-1/DUSP1) is neuroprotective in Huntington's disease via additive effects of JNK and p38 inhibition. J Neurosci 33:2313–2325. CrossRef Medline

Tecuapetla F, Matias S, Dugue GP, Mainen ZF, Costa RM (2014) Balanced activity in basal ganglia projection pathways is critical for contraversive movements. Nat Commun 5:4315. CrossRef Medline

Tian D, Litvak V, Lev S (2000) Cerebral ischemia and seizures induce tyrosine phosphorylation of PYK2 in neurons and microglial cells. J Neurosci 20:6478–6487. Medline

Tokiwa G, Dikic I, Lev S, Schlessinger J (1996) Activation of Pyk2 by stress signals and coupling with JNK signaling pathway. Science 273:792–794. CrossRef Medline

Trettel F, Rigamonti D, Hilditch-Maguire P, Wheeler VC, Sharp AH, Persichetti F, Cattaneo E, MacDonald ME (2000) Dominant phenotypes produced by the HD mutation in STHdh^{Q111} striatal cells. Hum Mol Genet 9:2799–2809. CrossRef Medline

Walker FO (2007) Huntington's disease. Lancet 369:218–228. CrossRef Medline

Yu H, Li X, Marchetto GS, Dy R, Hunter D, Calvo B, Dawson TL, Wilm M, Anderegg RJ, Graves LM, Earp HS (1996) Activation of a novel calcium-dependent protein-tyrosine kinase. Correlation with c-Jun *N*-terminal kinase but not mitogen-activated protein kinase activation. J Biol Chem 271:29993–29998. CrossRef Medline